Modeling of High Temperature GaN Quantum Dot Infrared Photodetectors

S. Razi [a], A. Asgari [a, b, *], and F. Ghasemi [a]

[a] Photonics Group, Research Institute for Applied Physics, University of Tabriz, Tabriz 51665-163, Iran

[b] School of Electrical, Electronic and Computer Engineering, The University of Western Australia, Crawley, WA 6009, Australia

*** Corresponding Author Email: asgari@tabrizu.ac.ir**

Abstract— In this paper, we present calculations for different parameters of quantum dot infrared photodetectors. We considered a structure which includes quantum dots with large conduction-band-offset materials (GaN/AlGaN). Single band effective mass approximation has been applied in order to calculate the electronic structure. Throughout the modeling, we tried to consider the limiting factors which decline high temperature performance of these devices. Temperature dependent behavior of the responsivity and dark current were presented and discussed for different applied electric fields. Specific detectivity used as figure of merit, and its peak was calculated in different temperatures. This paper indicates the state of the art in the use of the novel III-N materials in infrared detectors, with their special properties such as spontaneous and piezoelectric polarizations. It was found that, III- nitride Quantum dots have a good potential to depress the thermal effects in the dark current which yields the specific detectivity up to~ 2×10^7 $CmHz^{1/2}/W$ at room temperature.

KEYWORDS: Photo-detectors, GaN quantum dots, Temperature effects, Thermal effects.

I. INTRODUCTION

Detectors operating in the (3–25 μm) infrared regime have many applications including battlefield-imaging, medical applications, mine detection, remote-sensing and telecommunications. So there were special attentions for finding good detecting systems, for long years. Recently, the optical detectors based on quantum dots (QDs) attracted a lot of scientific attentions. The important features of these devices are, three dimensional quantum confinement, which results in the δ-like density of states [1] , [2], reduced electron-phonon scattering, so long excited state lifetime and high current gain, and their ability for operating at high temperatures [3], [4].These devices have great potential to overcome the drawbacks of the commercialized quantum well infrared photodetectors (QWIPs). In order to improve the performance of these detectors, different structures and materials have been investigated until now [5]-[7]. In the past decade, Wurtzite III-nitride quantum dots (QDs) have been extensively studied for their potential use, in different optoelectronic devices. GaN and its alloys with AlN, have strange properties such as, larger saturation velocity, large band gap and higher thermal stability, in comparison to the usual and prevalent, III-V materials [8]. But unfortunately, they still, suffer from a certain lack of knowledge, in terms of fundamental material parameters, and, they are in their early stage. Here we tried to investigate QDs with these novel materials, which may be useful, in high temperature performances, of these kinds of detectors.

In this paper the detector parameters such as responsivity and dark current were evaluated precisely, by considering their temperature dependence. Specific detectivity used as figure of merit, and its peak was calculated as function of temperatures for different applied bias.

II. THEORY AND DISCUSSIONS

A cuboid shape GaN QD, which has been surrounded by $Al_{0.2}Ga_{0.8}N$ barriers, has been considered as a unit cell. The proposed QD structure has been shown in Fig. 1. Five layers with doping density of $2\times10^{18}\,cm^{-3}$, QD density of $Nd=10^{24}\,m^{-3}$ are used as the active region of the device.

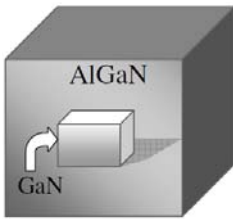

Fig. 1 The proposed cuboid shaped GaN QD within a $Al_{0.2}Ga_{0.8}N$ layer.

In order to calculate the eigen function and eigen values of the confined electrons, in QDs, we had to solve the Schrödinger equation. Different methods have been used to solve Schrödinger equation until now. Comparisons between single band, eight band k.p and the more accurate direct diagonalization empirical pseudo potential method (DD-EPM) were reported in [9]. It was shown that the commonly used eight band k.p model which has been used by different authors [10], [11], did not fare significantly better in terms of accuracy, for determining the electronic band structures. Here, we used single band effective mass approximation, and calculated the electronic structure precisely. It should be mentioned that the embedding technique has been successfully used previously, by number of authors [12]-[15]. In the frame work of the envelope function and the effective mass theory, the Hamiltonian can be written as [12]:

$$H=\frac{-\hbar^2}{2}\nabla\frac{1}{m^*(x,y,z)}\nabla+V(x,y,z), \qquad (1)$$

where,

$$m^*(x,y,z)=\begin{cases} m^*_{GaN} & in\,QD \\ m^*_{AlGaN} & else \end{cases}, \qquad (2)$$

$$V(x,y,z)=\begin{cases} 0 & in\ QD \\ \Delta E_c\ or\ \Delta E_v & else \end{cases}. \qquad (3)$$

in which m^*_{GaN} and m^*_{AlGaN} are the effective mass of electrons in GaN and AlGaN respectively, and ΔE_c, *and* ΔE_v are the conduction band and valance band discontinuity, respectively. As we only consider the transitions in the conduction band, so we have considered only the conduction band discontinuity [16]:

$$\Delta E_c=0.7\left(6.13x+3.42(1-x)-x(1-x)-E_{g0}\right)\text{eV} \qquad (4)$$

where E_{g0} is the GaN band gap, and x notifies Al- molar fraction in the barrier, and has been considered 0.2 in our calculations. As the system should be under bias in order to collect the Photo-excited carriers, the Hamiltonian should be modified as:

$$H=\frac{-\hbar^2}{2}\nabla\frac{1}{m^*(x,y,z)}\nabla+V(x,y,z)+e\mathbf{F}\cdot\mathbf{r}. \qquad (5)$$

where **F** demonstrates both the external and built in electric fields. It should be mentioned that III- nitrides in the wurtzite phase, have a strong spontaneous macroscopic polarizations and large piezoelectric coefficients. The abrupt variation of the polarization at interfaces, gives rise to a large polarization sheet charges which, in turn, creates a noticeable built-in electric field [17]. Therefore, the optical properties of wurtzite AlGaN/GaN QDs are affected by the 3D confinement of electrons and holes, and the strong built-in electric field in the QDs region, which in turn, causes simulation of these systems, extremely challenging task.

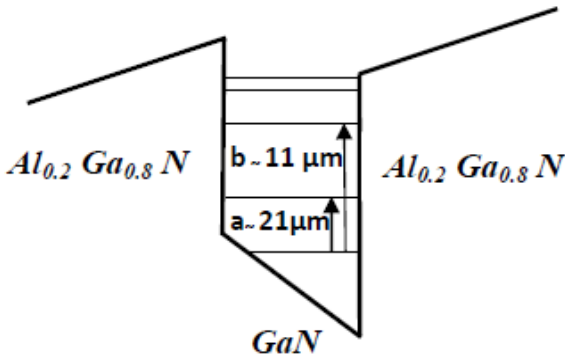

Fig. 2 Energy diagram for the proposed structure, and the possible transitions, 'a' and 'b'. (l_x=l_y=9nm, and l_z=3nm)

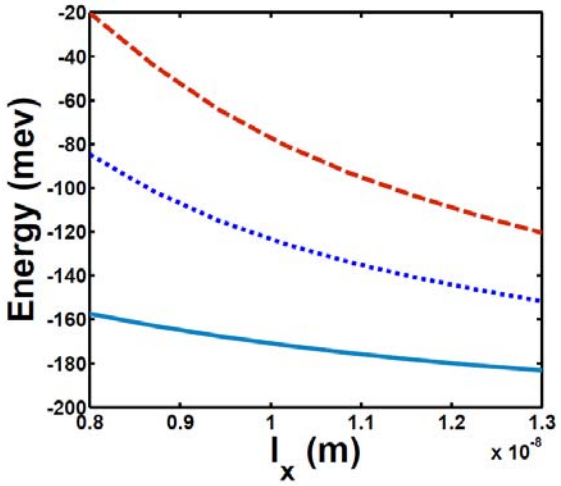

Fig. 3 Ground state, first and second excited states of the unit cell as a function of l_x with l_z=3nm.

The relations for the Built in electric field, piezoelectric polarizations and the approaches for solving the Schrödinger equation could be found in our previous successful work [18] and all other material parameters could be found in [19]. We should emphasize, although the equation of Built in electric field is in one dimensional, but we have considered it in 3D by substituting the amounts of each direction in every stage it should be mentioned that as reported in [20] the attraction of the normalized plane wave approach, lies in the fact that, there is no need to explicitly match the wave functions, across the boundary of the barrier and QD materials. Hence this method is easily applied to an arbitrary confining potential problem. As more plane waves were taken, more accurate results were anticipated. We used nine normalized plane waves in each direction to form the Hamiltonian matrix (i.e. n_x, n_y, and n_z from -4 to 4) and we formed 729*729 matrix. It was found that using more than 9 normalized plane waves in each direction takes significantly long computational time and only about 1 meV more accurate energy eigenvalues. The energy Eigenvalues of the considered structure have been demonstrated in Fig. 2. Ground state, first and second excited states of the unit cell as a function of dimension, has been illustrated in Fig. 3. Results indicate how these levels, by increasing the QD size, behave.

The oscillator strength, f_{if}, which is one of the most important factors controlling the absorption coefficient, $\alpha(\omega)$, can be written as:

$$f_{if} = \frac{2m^*}{\hbar^2}\left(E_i - E_f\right)\left|\mathbf{r}_{if}\right|^2. \qquad (6)$$

in which $\mathbf{r}_{if}$ is the transition matrix element from initial state to the excited state, $r_{if} = <\psi_i | r | \psi_f>$, where ψ_i and ψ_f are the wave functions of the initial and final states, which obtained from Schrödinger equation. The high oscillator strength is always associated with transition to the state, directly above the initial one, with an s-symmetry to p-symmetry change. The oscillator strength for transition from ground state to the first excited state ('a' transition in Fig. 2) was calculated about 0.2. But as we looked for the transitions, in the range of 8-12 µm, we considered transition from ground state to the second excited state. The Oscillator strength for this transition (b transition in Fig. 2) was calculated and it is about 3×10^{-3}.

The absorption coefficient is given by:

$$\alpha = \frac{\pi\hbar N_d n_{op} e^2}{m^* \varepsilon\varepsilon_0 c} N_i \left(1-n_e\right) f_{if} \frac{\Gamma}{\left(\hbar\omega - \hbar\omega_{if}\right)^2 + \Gamma^2}, \qquad (7)$$

where Γ is the life time broadening which has been considered 3×10^{-3} eV. n_{op} Is the refractive index of QDs, ε_0 and ε are the permeability of the free space and the medium, respectively. N_i Is the occupation probability of the initial states, and N_i is given by [21]:

$$N_i = \frac{e^{-E_i/k_BT}}{\sum_s e^{-E_s/k_BT} + \int_{\varepsilon_c} d\varepsilon \rho(\varepsilon) f(\varepsilon)/N_d}. \quad (8)$$

where E_S indicate the quantum dot energy levels, $\rho(\varepsilon)$ is the density of continuum states, and k_B is Boltzmann constant. For the low temperatures, $N_i \approx 1$ and the specific transition is high, but with increasing the temperature, the carriers redistributed and the transition decreases.

The peak of the absorption coefficient for "b" transition is plotted in Fig. 4. Results indicate that the absorption coefficient is almost constant until ~100 K and decreases with further increasing the temperature. This is a very important result, which will affect the detector all parameters at high temperatures. This behavior seems to be correct, because: As the temperature increases, more electrons occupy the lower states of the quantum dots. As long as, there are unoccupied excited states available, the electrons in the lower states, can participate in photon induced intraband transitions. However, a further increase in the number of electrons in the quantum dots, which results from the increase in dark current at higher temperatures, will cause a decrease in the number of unoccupied excited states and, consequently, a decrease in the absorption coefficient.

Figure 5 indicates the behavior of optical absorption of the structure with different QD sizes for the transition indicated as "b" in Fig. 2. It is obvious that by increasing the size of QD, the peak of the absorption increases and there is a red shift which can be related to increasing of the oscillator strength, and decreasing of the energy levels difference, respectively.

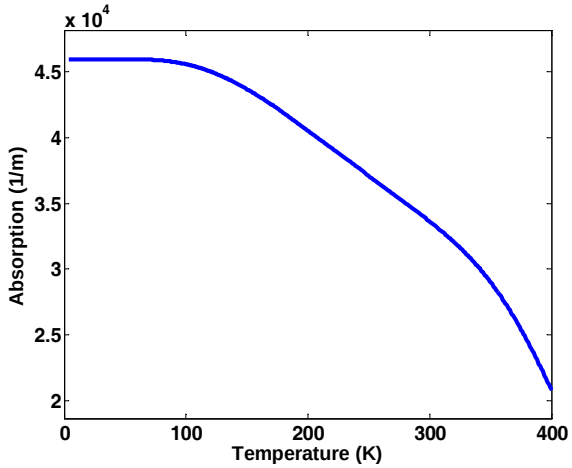

Fig. 4 The peak of absorption coefficient for the transition 'b' vs. temperature. The GaN QD size in x–y plane and z direction is considered (l_x=l_y=10nm, and l_z=3 nm), respectively.

As mentioned above, QD structures have long excited state lifetime, due to the reduced electron-phonon scattering. The long excited state lifetime not only allows efficient collection of Photo-excited carriers but also leads to high photoconductive gain and photo-responsivity [22]. The responsivity is one of the most important parameters of photodetectors which depends on gain and quantum efficiency.

The gain is defined as the ratio of the mean free path of the electron to the width of the sample, or the ratio of the recombination time to the transit time as:

$$g = \frac{\mu F}{LC_{be}}, \quad (9)$$

where, C_{be} is the quantum mechanical capture rate into the QD excited state. Estimates for the C_{be} in the literatures, are in the range of $\sim 10^{11} - 10^{12}$ Hz for shallow excited states, which are reachable by acoustic phonon emission, and is about $\sim 10^{10}$ for deep levels [23], [24]. μ is the mobility of the electron, which has been successfully demonstrated, in our previous work by considering all

scattering mechanisms, and the effects of temperature and electric fields [25].

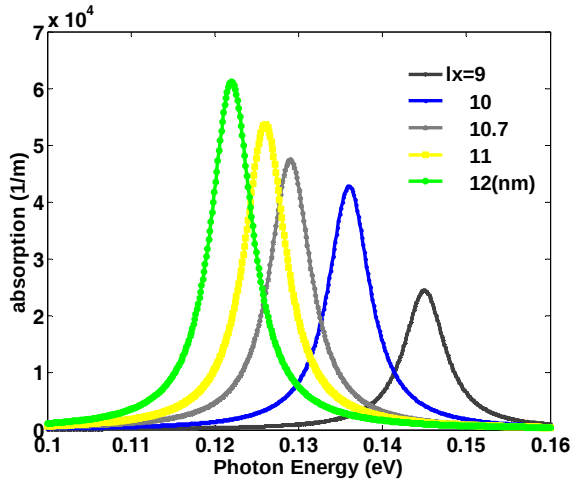

Fig. 5 The behavior of absorption vs. the photon energy for different QD sizes in T=77 K (l_x=l_y=10nm, and l_z=3nm).

The Quantum efficiency is defined as [26]:

$$\eta = \alpha(\omega) L \left(\frac{\nu_{ec} e^{-E_{ec}(F)/k_B T}}{\nu_0 + \nu_{ec} e^{-E_{ec}(F)/k_B T}} \right), \qquad (10)$$

where E_{ec} is the effective field dependent energy difference between the photo-excited state and the continuum ν_{ec} is the phonon assisted escape to continuum prefactor and expected to be weakly temperature dependent and is considered about $\sim 10^{13}$ Hz. ν_0 Is the relaxation rate from the photo-excited state to all other states and considered $\sim 10^{13}$ Hz and L is the device length in the 'Z' direction. Responsivity of the photodetector is the ratio of its output electrical signal, either as a current, I_{out}, or a voltage, V_{out}, to the input optical signal, expressed in terms of the incident optical power, P_{in}. By considering the relations (12) and (13) the responsivity can be written as:

$$R = \frac{e}{\hbar\omega} g\eta . \qquad (11)$$

By considering the normalized responsivity as,

$$R / R_0 = N_i \left(\frac{\upsilon_{ec} e^{-E_{ec}(F)/k_B T}}{\upsilon_0 + \upsilon_{ec} e^{-E_{ec}(F)/k_B T}} \right) F , \qquad [18]$$

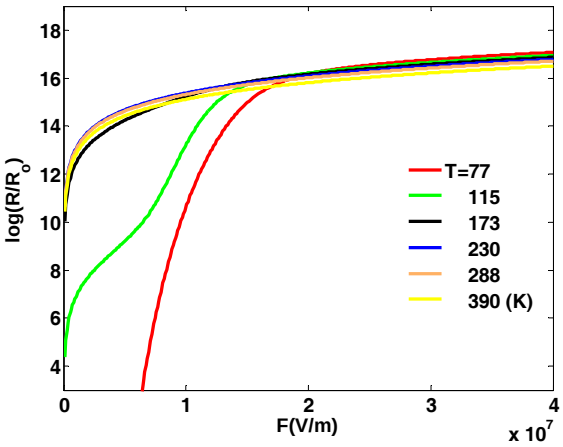

Fig. 6 The logarithm of normalized responsivity as a function of the external electric field for the different temperatures in GaN QDIP with (l_x=l_y=10nm and l_z=3nm).

In Fig. 6, the logarithm of the normalized responsivity versus applied fields for different temperature, for escape energy of ~30 meV, are presented. As depicted in the figure, for high electric fields, the normalized responsivity is almost independent of temperature.

Fig. 7 shows the normalized responsivity as a function of temperature, at several applied electric fields, for escape energy of ~30 meV. As expressed in the figure, the normalized responsivity has a maximum values for the temperature range of ~130-180 K. As can be deduced from the relations, there is two main sources for temperature dependence of the responsivity, current gain and quantum efficiency. It is well known that, there is a direct relationship between the maximum value of the absorption coefficient, and the quantum efficiency. Our calculations exhibit the reduction of the absorption coefficient with temperature. So the reduction of the quantum efficiency is expected, by increasing the temperature. It will decrease the responsivity in turn.

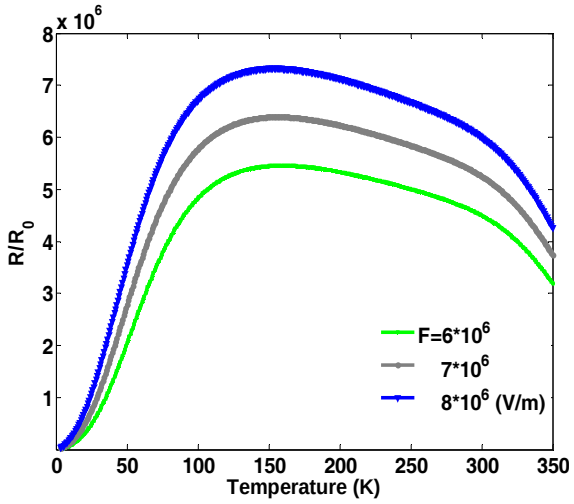

Fig. 7 Temperature dependent of the normalized responsivity for different external electric fields in GaN QDIP with (l_x=l_y=10nm and l_z=3nm).

Wang *et al.* have discussed temperature dependent behavior of the responsivity of InAs/GaAs quantum dot infrared photodetectors intelligently, in their excellent publication [4]. They have illustrated that temperature dependant of the responsivity is mostly affected by the current gain. They have calculated dramatic change of the current gain, and tried to explain its behavior, by the repulsive coulomb potential of the extra carriers in the dots. It will cause the capture probability decrease, with temperature, which leads to enhancement of optical gain. However, this effect is not included in our calculations, due to having no explicit expression for the capture decrease in GaN structures. It is obvious that including this parameter in calculations leads to improving the optical responsivity. There is other superior publication [27], which indicates the increase of responsivity by temperature, but the important point is that, this investigation is until~190 K, but our calculations support higher temperatures until 300 K.

Therefore our rough and theoretical calculation indicates that, the increasing of the temperature increases the current gain as well the responsivity. With further increasing the temperature N_i starts to decrease, therefore the absorption coefficient and quantum efficiency decreases and it makes a reduction in the responsivity.

The most important parameter, which restricts the detectivity of the optical detectors, in high temperatures, is dark current. There are some good discussions about the dark current mechanisms, in the literatures [7], [28], [29]. In this paper we tried to develop the theory of the dark current using a rate equation approach similar to the ones in the literature [30], except that the capture C_{be} and escape rates W_{SC} between the band and quantum level 's' are treated as quantum mechanical rates and path sums. Therefore the general expression for the dark current can be written:

$$I_d = \frac{Ae\mu FN_d}{(1-n_e)C_{be}} \sum_s \frac{f_s w_{sc}}{\left(1+\frac{w_{sc} f_s}{(1-n_e)C_{be}}\right)}. \qquad (12)$$

where f_s is the Fermi distribution function for the s^{th} energy state, A is the illuminated area of the device, $(1-n_e)$ is the probability that the state is empty. w_{sc} is the escape rate from Photo-excited state to continuum [26].

By considering $I_0 = \frac{Ae\mu FN_d}{(1-n_e)C_{be}}$, the logarithm of the dark current versus applied electric field at different temperatures has been plotted in Fig. 8 and also the logarithm of normalized dark current versus temperature inverse for different applied electric field has been shown in Fig. 9. Results illustrate that, at low temperatures, the dark current increases rapidly as the bias is increasing. This can be attributed to the rapid increase of electron tunneling between the QDs. As the bias increases, more electrons occupy the quantum dots, which results an increase in the average sheet electron density. When a large fraction of the quantum-dot states are occupied, further increase in bias, does not significantly alter the sheet electron density. This causes a lowering of the energy barrier for injected electrons at the contact layers, and linearly decreases of the dark current activation energy, which results in the nearly exponential increase of the dark current. At high bias, the activation energy was close to $\sim k_B T$, which results in

high dark current, even at low temperature. It is deduced from the results that dark current truly activated at high temperatures. Although high values for C_{be} will decrease the gain, but have advantage that will decrease dark current too. So structures with high densities of QDs might be useful and have a better performance in suppressing the dark current effects. It should be mentioned that the proposed structure has a less dark current in comparison to the structures introduced in Ref [26], [31].This can be attribute to the materials which have been used in our considered cell. The development of high performance infrared detectors, therefore, still requires a better control of the physical properties of the quantum dots; these properties include dot size, density, and spatial distributions [32].

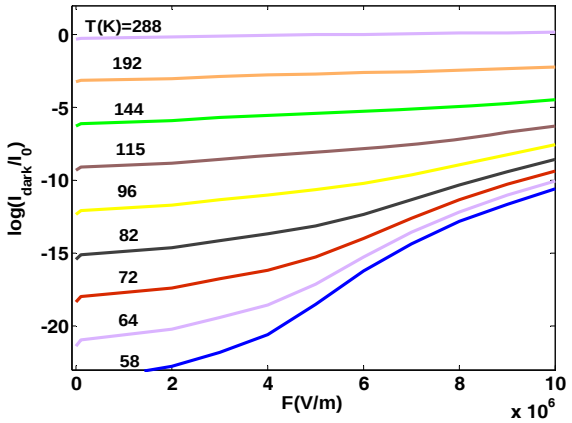

Fig. 8 The logarithm of the dark current versus external electric field for a GaN QDIP at different temperatures

Our calculations indicate a better result for the responsivity of this structure in comparison to our recent publication [18], in which we used a capping layer in the structure. So it demonstrates that in the structures with capping or blocking layer, for reaching an adequate responsivity, a higher bias should be imposed than the one, which have been used in this paper. But as it is evident from the Figs 8 and 9, the dark current is exceptionally bigger than the one in [18], so it is predicted that the specific detectivity will be very smaller than the structure including a capping layer [18].

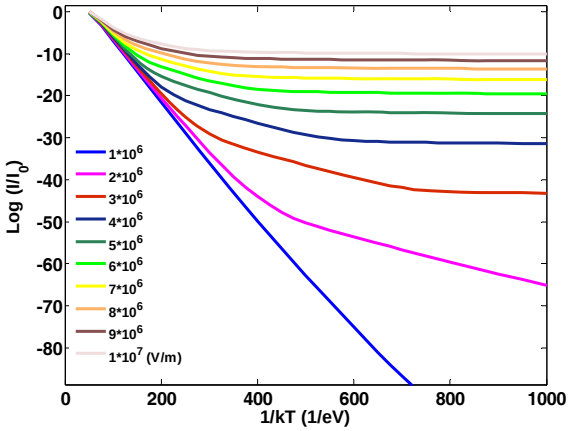

Fig. 9 The logarithm of the GaN QDIP dark current versus temperature inverse, $1/k_B T$. Each curve presents dark current in a fixed applied electric field.

Although the responsivity of a photodetector, gives the measure of the output signal of the detector, for a given optical input signal, but it does not give any information about the sensitivity of the device. The figure of merit used to evaluate the performance of most detectors, is the specific detectivity (D*), which is defined as [33]:

$$D^* = \frac{\text{Responsivity} \times \sqrt{A}}{\text{Noise}/\sqrt{\Delta f}} = \frac{R\sqrt{A\Delta f}}{i_N} \qquad (13)$$

In this relation i_N is the noise current and defines as $i_N = \sqrt{4eI_d g \Delta f}$, Δf is the band width frequency and we considered it ~ 1.

Fig. 10 indicates the variation of the specific detectivity with external electric field at T=66 K. One can observe that the increasing of the responsivity by the applied bias will increase the detectivity. By further increasing of the applied electric field, the raise of the dark current overcomes the responsivity, so the detectivity decreases. Fig. 11, shows temperature dependant of the specific detectivity, in the applied bias of $\sim 0.5V$.

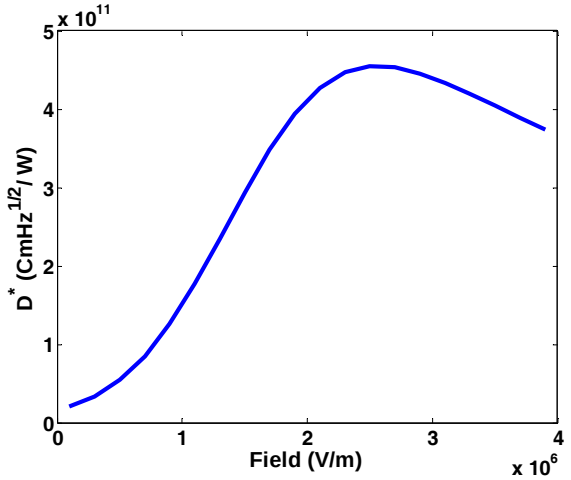

Fig. 10 The variation of the specific detectivity for GaN QDIP (lx=ly=10nm and lz=3nm) with external electric field in T=66 K.

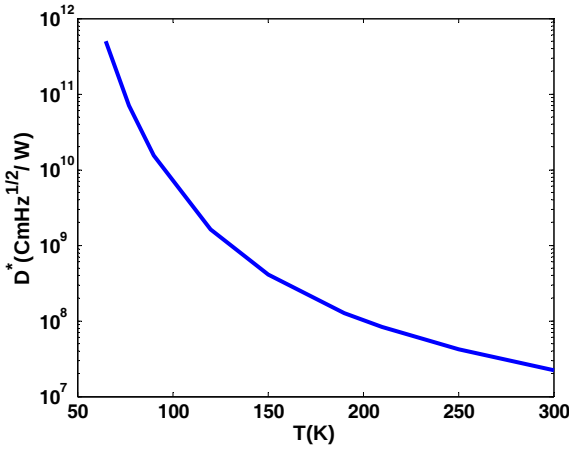

Fig. 11 The variation of the specific detectivity as a function of temperature for GaN QDIP (lx=ly=10nm and lz=3nm) in applied bias of 0.5 V.

The results are representative of high values for specific detectivity, in comparison to the similar structures which have been studied previously. Xuejun Lu *et al.* reported in [34], the peak specific photodetectivity of $3.8\times10^{9}\ cmHz^{1/2}/W$ and $1.3\times10^{8}\ cmHz^{1/2}/W$ at the detector temperature $T=78K$ and $T=170K$, respectively. Zhengmao Ye [35] give an account that for the photoresponse peaked at 6.2 μm and 77 K for -0.7 V bias, the responsivity was $14\ mA/W$ and the detectivity was $10^{10}\ cmHz^{1/2}/W$. Bhattacharya *et al.* [36] reported the some deal high detectivity, about $8.6\times10^{6}cmHz^{1/2}/W$, in $17\mu m$ wave length for 300 K temperature and in the other work they reported $6\times10^{9}\le D^{*}\left(CmHz^{1/2}/W\right)\le10^{11}$ for temperatures $100K\le T\le200K$ [37, 38].

III. CONCLUSION

As finding an appropriate material and structure, is the presentiment of the physicists or material scientists, here we tried to investigate nitride materials, which their specific properties, give hope to design detectors, with ability of working at high temperatures and in long wave length infrared. Temperature behaviour of detector parameters is the important aim of this work. So, the detector parameters, such as responsivity, dark current and the detectivity were evaluated precisely, by considering their temperature and field dependences. The structure studied is sufficiently general, so covers a large rang of possible device types. Due to better 3-D confinement of carriers, possibility of operating in high temperatures was observed. Although the results demonstrate a better amounts in both responsivity and detectivity for the considered structure in comparision to the III-V structures but it again approves the importance of using a capping and blocking layers in order to reach a higher detectivity in these detectors. Also the results indicate that the wide band gap and the large band offsets of the III-N systems give hope to band structure engineering for further improve of the detector parameters at high temperatures.

REFERENCES

[1] D. Pan, E. Towe, and S. Kennerly, "Normal-incidence intersubband (In, Ga) As /GaAs quantum dot infrared photodetectors," Appl. Phys. Lett. Vol. 73, pp. 1937-1938, 1998.

[2] L. Jiang, S. S. Li, N. Yeh, J. Chyi, C.E. Ross, and K.S. Jones, "$In_{0.6}Ga_{0.4}As$/GaAs Quantum dot infrared detector with operating temperature up to 260 K," Appl. Phys. Lett. Vol. 82, pp. 1986-1988, 2003.

[3] Z. Ye, J.C. Campbell, Z. Chen, E.-T. Kim, and A. Madhukar, "Noise and photoconductive gain in InAs quantum-dot infrared photodetectors," Appl. Phys. Lett. Vol. 83, pp. 1234-1236, 2003.

[4] S. Y. Wang, M. C. Lo, H. Y. Hsiao, H. S. Ling, C. P. Lee, "Temperature dependent responsivity of quantum dot infrared photodetectors," Infrared Physics & Technol, Vol. 50, pp. 166-170, 2006.

[5] S.Y. Lin, Y.R. Tsai, and S.C. Lee, "High-performance InAs/GaAs quantum-dot infrared photodetectors with a single-sided $Al_{0.3}$ $Ga_{0.7}$ As blocking layer," Appl. Phys. Lett., Vol. 78, pp. 2784-2786, 2001.

[6] H. Lim, W. Zhang, S. Tsao, T. Sills, J. Szafraniec, K. Mi, B. Movaghar, and M. Razeghi, "Quantum dot infrared photodetectors: Comparison of experiment and theory," Phys. Rev. B., Vol. 72, pp. 085332 (1-15), 2005.

[7] S.Y. Wang, S.D. Lin, H.W. Wu, C.P. Lee, "Low dark current quantum-dot infrared photodetectors with an AlGaAs current blocking layer,'' Appl. Phys. Lett. Vol. 78, pp. 1023-1025, 2001.

[8] N. Suzuki, N. Iizuka, and K. Kaneko, "simulation of ultrafast GaN/AlN intersub-band optical switches," IEICE Trans. Electron. Vol. E88-C, pp. 342-348, 2005.

[9] L.W. Wang, A.J. Williamson, A. Zunger, H. Jiang, and J. singh, "Comparison of the k_p and indirect diagonalization approaches to the electronic structure of InAs/GaAs quantum dots," Appl. Phys. Lett. Vol. 76, pp. 339-341, 2000.

[10] D.M.-T. Kuo and Y.C. Chang, "Effects of Coulomb blockade on the photocurrent in quantum dot infrared photodetectors," Phys. Rev B, Vol. 67, pp. 035313 (1-13), 2003.

[11] H. Jiang and J. Singh, "Conduction band spectra in self-assembled InAs/GaAs dots: A comparison of effective mass and an eight-band approach," Appl. Phys. Lett. Vol. 71, pp. 3239-3241, 1997.

[12] C.Y. Ngo, S.F. Yoon, W.J. Fan, and S.C. Chua, "Effects of size and shape on electronic states of quantum dots," Phys Rev B. Vol. 74, pp. 245331 (1-10), 2006.

[13] D. Gershoni, H. Temkin,G. J. Dolan, J. Duinsmuir, S.N.G. Chu, and M.B. Panish, "Effects of Two-Dimensional Confinement on the Optical Properties of InGaAs/InP Quantum Wire Structures," Appl. Phys. Lett. Vol. 53, pp. 995-997, 1988.

[14] M. Roy and P.A. Makasym, "Efficient method for calculating electronic states in self-assembled quantum dots," Phys .Rev. B, Vol. 68, pp. 235308 (1-7), 2003.

[15] M. Califano and P. Harrison, "Presentation and experimental validation of a single-band, constant-potential model for self-assembled InAs/GaAs quantum dots," Phys Rev B, Vol. 61, pp. 10959-10965, 2000.

[16] O. Ambacher, J. Smart, J.R. Shealy, R. Dimitrov, M. Stutzmann, and B.E. Foutz, "Two-dimensional electron gases induced by spontaneous and piezoelectric polarization charges in N- and Ga-face AlGaN/GaN heterostructures," J. Appl. Phys. Vol. 85, pp. 3222-3234, 1999.

[17] O. Mayrock, H.J. Wünsche, and F. Henneberger, "Polarization charge screening and indium surface segregation in (In,Ga)N/GaN single and multiple quantum wells," Phys. Rev. B, Vol. 62, pp. 16870-16880, 2000.

[18] A. Asgari and S. Razi, "High performances III-N Quantum Dot infrared photodetector operating in room temperature," Opt. Express, Vol. 18, pp. 1460414615, 2010.

[19] R. Cingolani A. Botchkarev, H. Tang, H. Morkoç, G. Traetta, G. Coli, M. Lomascolo, A. Di Carlo, F. Della Sala, and P. Lugli, "Spontaneous polarization and piezoelectric field in GaN/Al0.15Ga0.85N quantum wells: Impact on the optical spectra," Phys. Rev. B, Vol. 61, pp. 2711-2715, 2000.

[20] M.A. Cusack, P.R. Briddon, and M. Jaros, "Electronic structure of InAs/GaAs self-assembled quantum dots," Phys. Rev. B, Vol. 54, pp. R2300-R2303, 1996.

[21] M. Razeghi, H. Lim, S. Tsao, J. Szafraniec, W. Zhang, K. Mi, and B. Movaghar, "Transport and photodetection in self-assembled semiconductor quantum dots," Nanotechnol. Vol. 16, pp. 219-229, 2005.

[22] J. Liu, J. Bai, and G. Xiong, "Studies of the second-order nonlinear optical susceptibilities of GaN/AlGaN quantum well," Physica E, Vol. 23, pp. 70-74, 2004.

[23] J. Phillips, "Evaluation of the fundamental properties of quantum dot infrared detectors," J. Appl. Phys. Vol. 91, pp. 4590-4594, 2002.

[24] J.Z. Zhang and I. Galbraith, "Intraband absorption for InAs/GaAs quantum dot infrared photodetectors," Appl. Phys. Lett. Vol. 84, pp. 1934-1936, 2004.

[25] A. Asgari, M. Kalafi, and L. Faraone, "The effects of partially occupied sub-bands on two-dimensional electron mobility in AlxGa1-xN/GaN heterostructures," J. Appl. Phys., Vol. 95, pp. 1185-1190, 2004.

[26] H. Lim, J.Z. Zhang, and M. Razeghi, "Quantum dot infrared photodetectors: Comparison of experiment and theory," Phys. Rev. B. Vol. 72, pp. 085332-085347, 2005.

[27] X. Lu, J. Vaillancour, and M.J. Meisner, "Temperature-dependent photoresponsivity and high-temperature (190 K) operation of a quantum dot infrared photodetector," Appl. Phys Lett. Vol. 91, pp. 051115 (1-3), 2007.

[28] E. Towe and D. Pan, "Semiconductor quantum-dot nanostructures: Their application in a new class of infrared photodetectors," J. Selected Topics Quantum Electron. Vol. 6, pp. 408-421, 2000.

[29] V. Ryzhii, I. Khmyrova, V. Mitin, and M. Willander, "Device model for quantum dot infrared photodetectors and their dark-current characteristics," Semicond. Sci. Technol. Vol. 16, pp. 331-338, 2001.

[30] A.D. Stiff-Roberts, X.H. Su, S. Chakrabarti, and P. Bhattacharya, "Contribution of field-assisted tunneling emission to dark current in InAs-GaAs quantum dot infrared photodetectors," IEEE Photon. Technol. Lett. Vol. 16, pp. 867869, 2004.

[31] Z. Ye, J.C., Campbell, Z. Chen, E.-T. Kim, and A. Madhukar, "InAs quantum dot infrared photodetectors with $In_{0.15}Ga_{0.85}As$ strain-relief cap layers," J. Appl. Phys. Vol. 92, pp. 74627468, 2002.

[32] D. Pan, E. Towe, and S. Kennerly, "Normal-incidence intersubband (In, Ga)As/GaAs quantum dot infrared photodetectors," Appl. Phys. Lett. Vol. 75, pp. 1937-1939, 1998.

[33] R.V. Shenoi, R.S. Attaluri, A. Siroya, J. Shao, Y.D. Sharma, A. Stintz, T.E. Vandervelde, and S. Krishnab, "Low-strain InAs/InGaAs/GaAs quantum dots-in-a-well infrared photodetector," J. Vac. Sci. Technol. B, Vol. 26, pp. 1136-1139, 2008.

[34] X. Lu, J. Vaillancourt, M.J. Meisner, and A. Stintz, "Long wave infrared InAs-InGaAs quantum-dot infrared photodetector with high operating temperature over 170 K," J. Phys. D: Appl. Phys. 40, 5878, 2007.

[35] Z. Ye, J.C. Campbell, Z. Chen, E.-T. Kim, and A. Madhukar, "Normal-Incidence InAs Self-Assembled Quantum-Dot Infrared Photodetectors With a High Detectivity," IEEE J. Quantum Electron. Vol. 38, pp. 1234-1237, 2002.

[36] P. Bhattacharia and X.H. Su, "Characteristics of a tunneling quantum-dot infrared photodetector operating at room temperature," Appl. Phys. Lett. Vol. 86, pp. 191106-191108, 2005.

[37] A.D. Stiff, S. Krishna, P. Bhattacharya, and S.W. Kennerly, "Normal-Incidence, High-Temperature, Mid-Infrared, InAs/GaAs Vertical Quantum-Dot Infrared Photodetector," IEEE J. Quantum Electron. Vol. 37, pp. 1412-1419, 2001.

[38] S. Chakrabarti, A.D. Stiff-Roberts, P. Bhattacharia, S. Gunapala, S. Bandara, S.B. Rafol, and S.W. Kennerly, "High-temperature operation of InAs-GaAs quantum-dot infrared photodetectors with large responsivity and detectivity," IEEE Photon. Technol. Lett. Vol. 16, pp. 1361-1363, 2004.